Geometry Dependence of CMOS-Compatible, Polysilicon, Leaky-Mode Photodetectors

Robert Pownall, *Student Member, IEEE*, Guangwei Yuan, *Student Member, IEEE*, Tom W. Chen, *Senior Member, IEEE*, Phil Nikkel, and Kevin L. Lear, *Member, IEEE*

***Abstract*—Complementary metal–oxide–semiconductor-compatible metal–semiconductor–metal polysilicon photodiodes fabricated in a commercial 0.35-μm technology offer estimated responsivities of up to 0.35 A/W at 654 nm. An effective absorption coefficient of 0.63 dB/μm was extracted from responsivities for 5- to 10-μm-long waveguide-coupled detectors. Increasing responsivity at smaller contact spacing indicated a two-part photocurrent response, with secondary photocurrent dominating at small contact spacings and high electric fields.**

***Index Terms*—Complementary metal–oxide–semiconductor (CMOS)-compatible optoelectronic integrated circuits, leaky-mode metal–semiconductor–metal (MSM) photodiodes, optical interconnects, photoconductivity, waveguides.**

I. Introduction

THE effects of increased signal latency and increased global interconnect length on each microprocessor generation, resulting in worsening clock skew, timing delay, and jitter, as well as factors such as power consumption and area, are driving the investigation of optical interconnect technologies for on-chip use [1]. This letter reports the geometry dependence of polysilicon photodiodes for complementary metal–oxide–semiconductor (CMOS)-compatible on-chip optical interconnects.

While many promising proposals for on-chip optical interconnect technologies have been reported in the literature, such as those using embedded detectors [2] or polymer waveguides [3], they suffer from the drawback of incorporating processing or materials which are not part of industry-standard CMOS processes. Trench photodetectors [4] do use industry-standard CMOS techniques, but are aimed at surface normal incidence. In addition, they occupy valuable silicon surface area, and require the space above the trench to be kept free from metal lines and other circuitry so that vertically incident light can reach the detector.

The devices described in this letter, in contrast to [1]–[3], use only materials and processing which exist in standard commercial CMOS technologies [5]. As opposed to [4], these detectors can be placed at any point in the backend of the process and do not occupy substrate area, although a low-temperature polysilicon or amorphous silicon deposition is required for detectors positioned after first level metal.

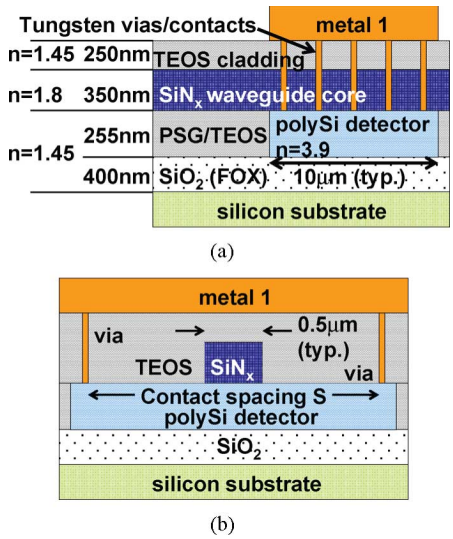

Fig. 1. Detector (a) side- and (b) end-view cross-sections.

While defects at grain boundaries of the polysilicon may raise concerns about recombination lifetimes, the reduced crystallinity also offers absorption that is approximately twice that of single-crystal silicon, or higher [6], [7]. While others have reported implant damaged crystalline silicon waveguide photodiodes [8] as well as polysilicon normal incidence photodiodes [9], these are believed to be the first waveguide coupled polysilicon photodetectors. The data presented below indicate that relatively short detectors have sufficient absorption and that smaller gap devices can provide larger responsivities via secondary photocurrents.

II. Fabrication

The wafers were fabricated at a commercial CMOS facility (Avago Technologies, Fort Collins, CO) in a 0.35-μm technology on 6-in wafers. After a 500-nm $n = 1.45$ field oxidation, a standard production process flow followed: 255-nm $n = 3.85$ polysilicon deposition (to serve as the detector layer); 120-nm $n = 1.80$ low-pressure chemical vapor deposition (LPCVD) nitride spacer layer; a second 20-nm $n = 1.80$ LPCVD nitride layer; 200-nm $n = 1.45$ phosphosilicate glass (PSG) deposition; PSG densification and 440-nm $n = 1.45$ tetraethyl ortho-silicate (TEOS) deposition. All thicknesses and refractive indexes listed here and shown in Fig. 1 are nominal values.

Manuscript received September 5, 2006; revised December 7, 2006. This work was supported by the National Science Foundation (NSF) GOALI Program under Contract ECS-0323493.

R. Pownall, G. Yuan, T. W. Chen, and K. L. Lear are with Colorado State University, Fort Collins, CO 80523-1373 USA (e-mail: Bob.Pownall@colostate.edu).

P. Nikkel is with Avago Technologies, Fort Collins, CO 80525 USA.

Color versions of one or more of the figures in this letter are available online at http://ieeexplore.ieee.org.

Digital Object Identifier 10.1109/LPT.2007.893573

Following the deposition and chem-mechanical polishing (CMP) of the initial intermetal TEOS dielectric, a 350-nm $n = 1.8$ plasma-enhanced chemical vapor deposition (PECVD) silicon nitride film was deposited, patterned, and etched, to serve as the core of the waveguide structure. This PECVD silicon nitride was a minor modification of a standard nitride deposition, and is slightly less dense than the earlier LPCVD nitride layers. The use of polysilicon as the detector layer provides a material with a refractive index higher than silicon nitride, permitting the desired leaky-mode coupling from the nitride waveguide core to the detector, while maintaining mechanical and thermal compatibility with the other films in the structure.

Following the waveguide creation step, an $n = 1.45$ TEOS layer was deposited and thinned, by CMP, to a nominal thickness of 280 nm over the waveguide nitride, before definition of the contacts and first level metal. The contacts are plugged with tungsten. The metal stack consisted of a 10-nm Ti layer, then a 390-nm Al/0.5% Cu layer, with a 35-nm TiN layer on top. After dicing, selected die were edge polished to an optical-quality finish, to allow end-fire coupling to the waveguide.

The design variables for the detectors themselves were the contact spacing, the detector length, and the waveguide width. Contact spacing S varied in somewhat logarithmic steps from 1.14 to 30.6 μm. Detector length L was limited to two values: 5 and 10 μm. This 2 : 1 ratio allowed for analytic extraction of the absorption coefficient of the polysilicon detector as described below. While detectors with a variety of waveguide widths were fabricated, only ones with single-mode 0.5-μm-wide waveguides are discussed here in order to maintain uniform coupling efficiency.

III. Experimental Procedure

Following polishing, dc characteristics of photodetectors with varying contact spacing and length values on the same die were measured. The sample was electrically probed while light from a $\lambda = 654$ nm laser diode was coupled to the waveguide via a 4-μm core diameter, 0.11 numerical aperture (NA) visible single-mode fiber with a cleaved end close to the polished chip facet. The fiber was actively aligned to the waveguide by initially biasing the photodetector under test at +5 V and maximizing the photocurrent. The bias voltage was swept from −20 to +20 V while measuring the photocurrent using a 267-ms integration time. Dark current for each photodetector was measured over the same bias range.

Input optical power was estimated by coupling light into a 0.5-μm waveguide that crossed the die without being coupled to an on-chip detector. Scattered intensity was measured by scanning a 62.5-μm core diameter fiber 25 μm above the surface of the waveguide and fit to determine waveguide loss. Based on the loss as well as the output power of the waveguide, the typical power in the waveguide immediately prior to the photodetector was estimated to be $P_{\text{inc}} = 5.3\ \mu$W.

IV. Experimental Results

The multiple of two in detector lengths (5 μm, 10 μm), combined with the standard exponential absorption model, results

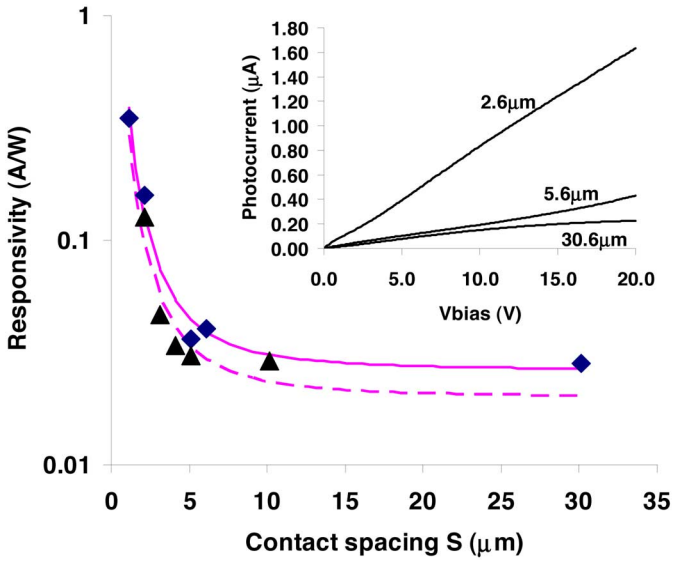

Fig. 2. Experimental data for 10-μm devices (diamonds) and fit to theory (solid line) for values in text. The 5-μm devices (triangles, dashed line) are also shown. V_{bias} is 10 V. The inset shows I–V characteristics for selected 10-μm-long detectors.

in a quadratic equation that can be solved to find the effective absorption rate

$$\alpha_{\text{eff}} = \frac{1}{L} \ln \left(\frac{2\rho}{1 - \sqrt{\frac{1-4\rho(1-\rho)}{(1-f)}}} \right). \tag{1}$$

Using $f = 0.355$ from [5] (f is the fraction of the incident power that is directly coupled from the waveguide into guided modes of the polysilicon), $L = 5\ \mu$m (the short detector length), and $\rho = 0.81$ as the average ratio of photocurrent of 5- and 10-μm-long detectors for the 2.6- and 5.6-μm contact spacings, the calculated effective absorption coefficient is 0.63 dB/μm, in good agreement with [5].

The dependence of photocurrent on contact spacing and applied voltage indicated that photoconductive gain was significant at E-fields above 10 kV/cm. As expected, reducing the contact spacing increased the responsivity for both 5- and 10-μm -long detectors as shown for a fixed bias of +10 V in Fig. 2. Other bias voltages had similar trends. No saturation of gain as a function of contact spacing was observed at the smallest contact spacing, indicating that yet smaller contact spacings will result in higher effective responsivity. The observed behavior is consistent with the known behavior of primary and secondary photocurrent resulting from a photoconductive gain process which is proportional to the ratio of carrier recombination lifetimes to transit time between the electrodes of the device [10].

The primary photocurrent is given by

$$I_1 = \eta_c \left[\frac{q\lambda}{hc} \right] P_{\text{opt}} \tag{2}$$

where η_C is the primary carrier collection efficiency and P_{opt} is the incident optical power. The primary photocurrent is largely independent of the applied field, as long as the field strength is sufficient to separate the photogenerated holes and electrons before they can recombine with each other. The photocurrent

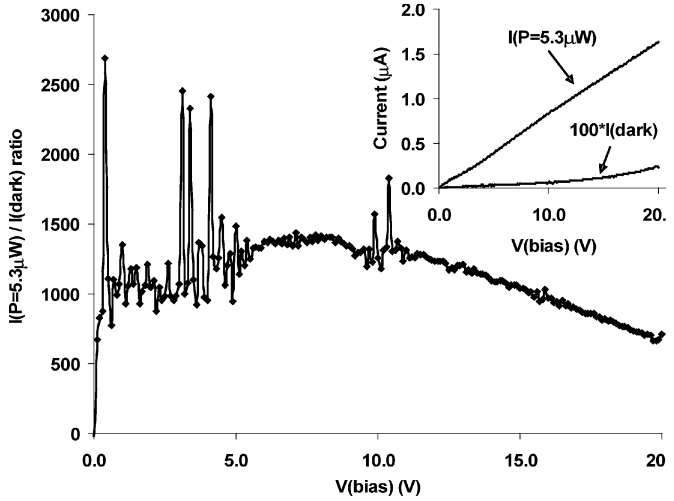

Fig. 3. Photocurrent to dark current ration for a 0.5-μm waveguide, 10-μm detector, 2.6-μm contact spacing device. Inset shows I–V characteristics for the same device. Noise spikes are due to instrument quantization noise when measuring dark current.

response shown in Fig. 2 for devices with 6-μm contact spacing or greater is mostly due to primary photocurrent.

The total photocurrent is given by the sum of primary and secondary photocurrent [10], [11]

$$I_{\rm ph} = I_1 \left(1 + \frac{\tau\,(\mu_n + \mu_p)\,V}{S^2}\right) \tag{3}$$

where μ_n and μ_p are the carrier mobilities, τ is the lifetime, and S is the contact spacing. This matches the observed behavior in Fig. 2. For the 10-μm-long devices and $P_{\rm inc} = 5.3\ \mu$W, an I_1 of 0.139 μA ($R_1 = 0.026$ A/W) and a $\tau(\mu_n + \mu_p)$ of 1.79 μm^2/V at $V = 10$ V fits the data well. With the same $\tau(\mu_n + \mu_p)$, the 5-μm I_1 is 0.106 μA ($R_1 = 0.0200$ A/W). The photoconductive gain process may slow the detectors; however, transient simulations of polysilicon detectors with Schottky contacts predict a -3-dB bandwidth of 7.9 GHz [12]. Experiments to measure pulsed response are planned for future work and will be reported when available. As shown in Fig. 2, and as expected from the detector length and contact spacing results, the 0.5-μm-wide waveguide, 10-μm-long detector, and 2.6-μm contact spacing device had the highest responsivity, at 0.16 A/W at 10 V. Our earlier work [5], which examined only 10-μm-long 1.14-μm contact spacing detectors in a clock-distribution H-tree, reported a responsivity of 0.35 A/W at 10 V.

Fig. 3 shows that the $I_{\rm ph}$ to dark current ratio, which is important for noise and signal detection threshold considerations, is above 500 and generally above 1000.

V. Conclusion

Responsivities of up to 0.35 A/W on unoptimized CMOS-compatible detectors have been measured. Responsivity can be increased by shrinking the contact spacing to increase the electric field, thus enhancing secondary photocurrent gain. An effective absorption coefficient of 0.63 dB/μm was extracted from the photocurrent ratio of two different lengths of detectors, indicating relatively short 10-μm-long detectors absorb most of the incident light. The $I_{\rm ph}/I_{\rm dark}$ ratio of $>$500 at modest incident powers offers excellent signal contrast.

Acknowledgment

The authors would like to thank R. Kee and B. Lewis of Avago Technologies for assistance in sample preparation

References

[1] E. Cassan, D. Marris, M. Rouviere, L. Vivien, and S. Laval, "Comparison between electrical and optical global clock distributions for CMOS integrated circuits," *Opt. Eng.*, vol. 44, pp. 105402-01–105402-10, 2005.

[2] N. A. Jokerst, T. K. Gaylord, E. Glytsis, M. A. Brooke, S. Cho, T. Nonaka, T. Suzuki, D. L. Geddis, J. Shin, R. Villalaz, J. Hall, A. Chellapa, and M. Vrazel, "Planar lightwave integrated circuits with embedded actives for board and substrate level optical signal distribution," *IEEE Trans. Adv. Packag.*, vol. 27, no. 2, pp. 376–385, May 2004.

[3] M. Siegert, M. Loken, C. Glingener, and C. Buchal, "Efficient optical coupling between a polymeric waveguide and an ultrafast silicon MSM photodiode," *IEEE J. Sel. Topics Quantum Electron.*, vol. 4, no. 6, pp. 970–974, Nov./Dec. 1998.

[4] M. Yang, K. Rim, D. L. Rogers, J. D. Schaub, J. J. Welser, D. M. Kuchta, D. C. Boyd, F. Rodier, P. A. Rabidoux, J. T. Marsh, A. D. Ticknor, Q. Y. Yang, A. Upham, and S. C. Ramac, "A high-speed, high-sensitivity silicon lateral trench photodetector," *IEEE Electron Device Lett.*, vol. 23, no. 7, pp. 395–397, Jul. 2002.

[5] G. Yuan, R. Pownall, P. Nikkel, C. Thangaraj, T. W. Chen, and K. L. Lear, "Characterization of CMOS compatible waveguide-coupled leaky-mode photodetectors," *IEEE Photon. Technol. Lett.*, vol. 18, no. 15, pp. 1657–1659, Aug. 1, 2006.

[6] Y. Laghla, E. Scheid, H. Vergnes, and J. P. Couderc, "Electronic properties and microstructure of undoped, and B- or P-doped polysilicon deposited by LPCVD," *Solar Energy Mater. Solar Cells*, vol. 48, pp. 303–314, 1997.

[7] D. P. Poenar and R. F. Wolffenbuttel, "Optical properties of thin-film silicon-compatible materials," *Appl. Opt.*, vol. 36, pp. 5122–5128, 1997.

[8] A. P. Knights, J. D. B. Bradley, S. H. Gou, and P. E. Jessop, "Silicon-on-insulator waveguide photodetector with self-ion-implantation-engineered-enhanced infrared response," *J. Vac. Sci. Technol. A*, vol. 24, pp. 783–786, 2006.

[9] R. P. MacDonald, N. G. Tarr, B. A. Syrett, S. A. Boothroyd, and J. Chrostowski, "MSM photodetector fabricated on polycrystalline silicon," *IEEE Photon. Technol. Lett.*, vol. 11, no. 1, pp. 108–110, Jan. 1999.

[10] S. L. Chuang, *Physics of Optoelectronic Devices*, 1st ed. New York: Wiley, 1995, pp. 585–587.

[11] R. H. Bube, *Photoconductivity of Solids*, 2nd ed. Huntington, NY: Krieger, 1978, pp. 75–77.

[12] A. M. Raza, "A Truly CMOS Compatible Waveguide Coupled Photodiode for On-Chip Optical Interconnects," Master's, Dept. Elect. and Comput. Eng., Colorado State Univ., Fort Collins, CO, 2005.